JOURNAL OF MATERIALS SCIENCE 31 (1996) 2279–2289

Corrosion behaviour of steel in high alumina cement mortar cured at 5, 25 and 55 °C: chemical and physical factors

A. MACIAS
Instituto de Ciencias de la Construccion, Eduardo Torroja, Madrid, Spain
A. KINDNESS, F. P. GLASSER
University of Aberdeen, Aberdeen, UK

The corrosion behaviour of embedded steel was related to the composition of the pore phase in equilibrium with the hydrated phases and the porosity of the high alumina cement mortars subsequent to curing at 5, 25 and 55 °C. The corrosion of reinforcements was evaluated by electrochemical techniques. The effect on corrosion of 3% by weight of cement of NaCl, added during the mixing process, and of the accelerated carbonation of mortars in CO_2 atmosphere were also determined. The pH value and the chemical composition of pore fluid of plain high alumina cement (HAC) mortar cured at all three temperatures suggested that the embedded steel was in a passivated state. The resistance of HAC to carbonation and its greater potential for chloride binding by chloroaluminate formation are believed to make HAC inherently more protective to steel, relative to normal Portland cement, during ingress of chloride from external sources. High corrosion rates reported in literature for steel embedded in HAC may be attributable to bad practice, not to lack of passivity.

1. Introduction

Although structural uses of high alumina cement (HAC) are severely restricted, mainly due to loss of strength caused by conversion of hexagonal to cubic calcium aluminate hydrate and the associated increase of porosity, many structures remain and continue to give satisfactory service. The durability of HAC in the marine environment assures its continuing use; moreover, blends of HAC with slag appear to be resistant to conversion [1] and offer possible re-entry of HAC to the family of acceptable constructional materials.

HAC concretes have lower pore solution pHs than those of equivalent Portland cement formulations, which might imply less corrosion protection to embedded steel. However, deleterious chloride may be better bound in HAC as Friedel's salt on account of the high aluminate content of HAC. Relatively little research exists on either this binding potential or on the corrosion behaviour of reinforcement in HAC [2, 3].

The aim of this work is to analyse the chemical and physical factors relevant to corrosion behaviour of steel in a HAC mortar, in particular the composition of the pore phase in equilibrium with the hydrated phases subsequent to curing at 5, 25 and 55 °C, as well as the porosity of the respective mortars. The effect of 3% by weight of cement of NaCl, added during the mixing process, and of the accelerated carbonation of mortars in a CO_2 atmosphere were also studied. The chloride binding potential of the aluminates will be described in a subsequent publication.

2. Experimental procedure

2.1. Materials and procedure

HAC with the oxide composition given in Table I was employed to prepare mortar cylinders 42 mm diameter × 85 mm length for pore fluid expression studies. The cylinders had a water/cement (w/c) ratio of 0.6 and cement/sand ratio of 1 : 1. The high w/c ratio was chosen to accelerate reaction during subsequent carbonation and to facilitate collection of sufficient pore fluid for chemical analysis.

Chloride additions were made by adding NaCl to the mix water.

The samples were demoulded within a few hours and thereafter moist cured at 5, 25 and 55 °C. After 14 days cure, one set of samples was placed in a moist, 100% CO_2 atmosphere.

Two identical, chemically-cleaned steel bars, 1 cm diameter and 8 cm long with an exposed area of 17 cm^2, were embedded in the mortar cylinders for corrosion studies. A saturated calomel electrode and a graphite bar were employed as reference and auxiliary electrodes respectively. The minimum thickness of the cover was ca. 15 mm.

0022–2461

TABLE I Oxide composition of high alumina cement, wt%

CaO	SiO_2	Al_2O_3	Fe_2O_3	MgO	SO_3	Na_2O	K_2O
37.65	2.97	43.49	15.43	0.58	0.09	0.20	0.06

In order to study the solid phases by X-ray diffraction, a series of slabs of HAC pastes were prepared and cured under similar conditions.

2.2. Techniques used

Pore fluid expression was done by hydraulically compressing mortar cylinders, ca. 42 mm diameter, in an alloy steel jacket; ca. 100 t of force were available. The expressed fluid was collected directly into sample vials, assisted by an N_2 purge. The pore fluid was filtered through a 0.45 μm membrane filter and analysed as soon as practicable thereafter. The aqueous pH was measured both with a pH electrode and by titration with HCl using both methyl orange and phenolphthalein as indicators. Aqueous Ca^{2+} concentrations were determined by atomic absorption spectrometry; Na^+, K^+ and Al^{3+} by atomic emission spectrometry and Cl^- by titration.

The polarization resistance, R_p, was measured by plotting a polarization curve from -10 to $+10$ mV around the corrosion potential, E_{corr}, using a sweep rate of $10^{-4}\,V\,s^{-1}$. The corrosion intensity was calculated by Stern and Geary's formula [4]

$$i_{corr} = B/R_p \quad (1)$$

where the constant B is given by

$$B = \beta_a\beta_c/2.3(\beta_a + \beta_c)$$

where β_a and β_c are the Tafel slopes of the cathodic and anodic processes respectively. A constant B value of 26 mV was used when the bar was being actively corroded and 52 mV when passivated.

X-ray diffraction and mercury intrusion porosimetry were carried out with commercial instruments; a Philips PW1740 diffractometer and Micromeritics Pore Sizer 9300, respectively. DTA/TG measurements were carried out with a Netzsch simultaneous thermal analyser, in nitrogen atmosphere at a heating rate of $5\,°C\,min^{-1}$ from 0 to 1050 °C.

3. Results

3.1. Composition of solid phases

A summary of the phases identified by X-ray diffraction in pastes corresponding to the mortar cylinders of HAC is presented in Tables II and III. From these tables, and in agreement with the literature, the calcium aluminate hydrate mineralogy is temperature-dependent; HAC hydrates at 55 °C to yield mainly the stable cubic aluminate, C_3AH_6, whereas at 25 °C, mixtures of hexagonal hydrated aluminates, CAH_{10} and C_2AH_8, are obtained. At 5 °C, CAH_{10} is the principal hydrate.

Conversion of hexagonal phases to the more stable cubic phase occurs slowly at 25 °C but not at 5 °C over the duration of the experiments. However, Cl added as sodium chloride to the mix water, combines with Ca

TABLE II Summary of the phase development in HAC pastes (phase presented in order of decreasing proportion in the pastes)

		Phases found	
Sample	Temperature (°C)	~1 month cure	~4 months cure
HAC	55	C_3AH_6; AH_3; CC(t)	C_3AH_6; Mc; AH_3; CC(t)
HAC	25	CAH_{10}; Mc; C_2AH_8(t); CC(t); C	C_3AH_6; Mc(t); AH_3(t)
HACl	5	CAH_{10}; CA; CC(t)	CA; CAS; CC; CAH_{10}(t)
HAC + 3% NaCl	55	C_3AH_6; AH_3; FS	FS; C_3AH_6
HAC + 3% NaCl	25	CAH_{10}; CA; C_2AH_8; FS	C_3AH_6; FS; CAH_{10}(t)
HAC + 3% NaCl	5	CAH_{10}; CA; FS; Mc(t)	CAH_{10}; CAS; FS; CC; CA(t); AH_3(t)

$AH_3 = Al(OH)_3$; CA = $CaAl_2O_4$; CAS = calcium aluminium silicate; CC = $CaCO_3$; $CAH_{10} = CaAl_2(OH)_8\cdot 6H_2O$; $C_2AH_8 = Ca_2Al_2(OH)_{10}\cdot 3H_2O$; $C_3AH_6 = Ca_3Al_2(OH)_{12}$; FS = $Ca_4Al_2O_7Cl_2\cdot 12H_2O$; MC = $Ca_4Al_2O_7CO_3\cdot 11H_2O$.

TABLE III Summary of the phase development in carbonated HAC pastes (phase presented in order of decreasing proportion in the pastes)

		Phases found	
Sample	Temperature (°C)	15 days initial cure + 15 days CO_2	15 days initial cure + 3 months CO_2
HAC	55	CC; AH_3; C_3AH_6(t)	CC; AH_3(t)
HAC	25	CAH_{10}; CC; CA(t); C_2AH_8(t); AH_3(t)	CC
HAC	5	CAH_{10}; CA; CC(t)	CC; CAS; CAH_{10}(t); CA(t)
HAC + 3% NaCl	55	AH_3; CC; C_3AH_6; FS	CC
HAC + 3% NaCl	25	CC; CA; CAH_{10}; FS; AH_3(t)	C_3AH_6; CAH_{10}; FS
HAC + 3% NaCl	5	CAH_{10}; CA; CC; FS(t)	CAH_{10}; CC; CAS; CA(t); AH_3(t)

$AH_3 = Al(OH)_3$; CA = $CaAl_2O_4$; CAS = calcium aluminium silicate; CC = $CaCO_3$; $CAH_{10} = CaAl_2(OH)_8\cdot 6H_2O$; $C_2AH_8 = Ca_2Al_2(OH)_{10}\cdot 3H_2O$; $C_3AH_6 = Ca_3Al_2(OH)_{12}$; FS = $Ca_4Al_2O_7Cl_2\cdot 12H_2O$; MC = $Ca_4Al_2O_7CO_3\cdot 11H_2O$.

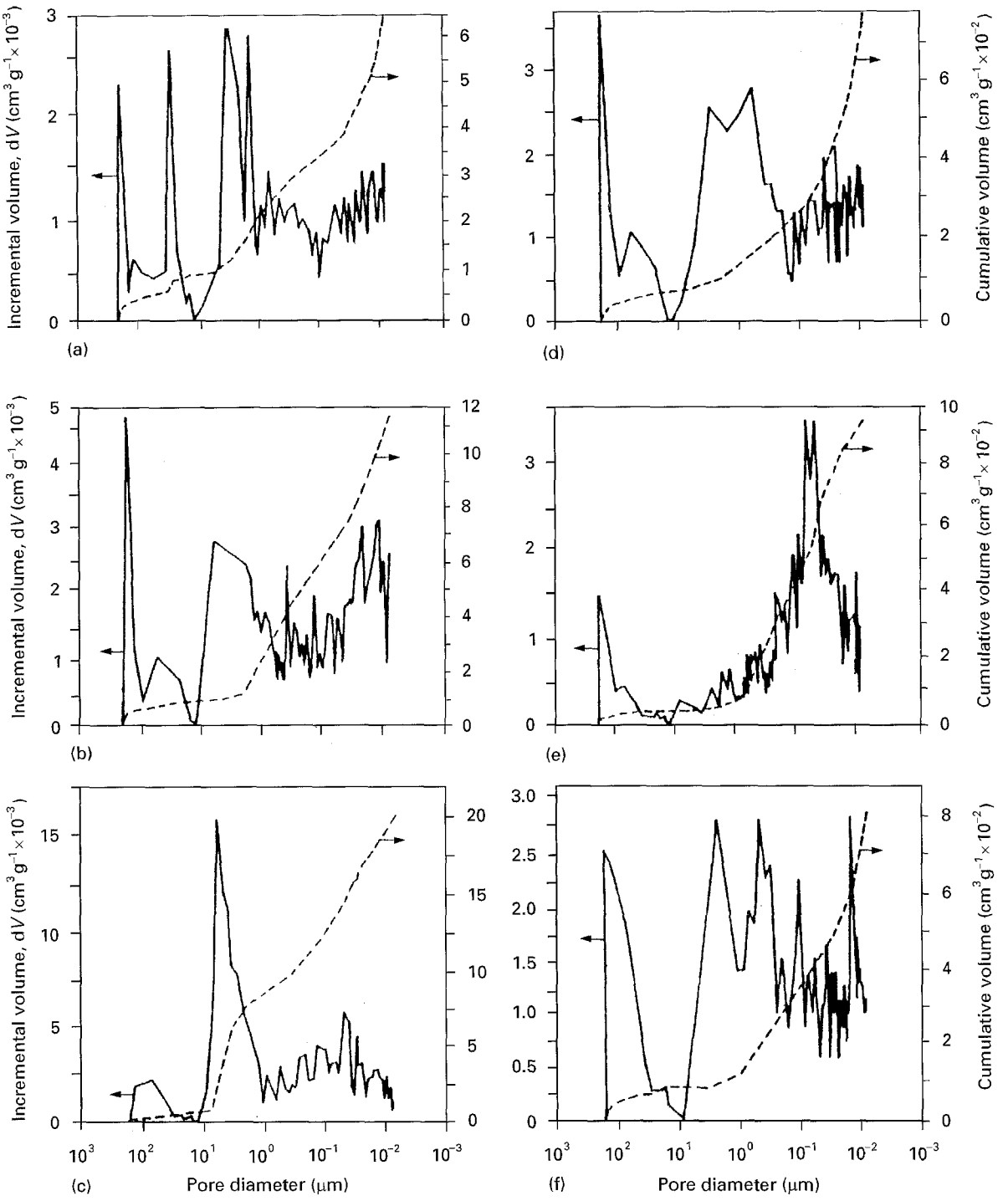

Figure 1 Incremental and cumulative pore volume as a function of the mean pore entry diameter for HAC mortar after ~4 months of curing at (a) 5, (b) 25 and (c) 55 °C and after 15 days initial cure and ~3 months carbonation at the same three temperatures (d–f).

and Al as Friedel's salt. Thus, the normal hydroxyaluminates characteristic of HAC are partly replaced by the chloroaluminate. Friedel's salt itself is destroyed by carbonation, especially in 55 °C cures.

3.2. Mercury intrusion porosimetry

Fig. 1 gives dV, the incremental and cumulative pore volume ($cm^3\,g^{-1}$) as a function of the mean pore entry diameter (μm) for HAC mortar cured at 5, 25 and 55 °C and after three months carbonation at the same three temperatures. The incremental volume plots show that the pore size distribution is shifted to a pore regime of smaller entry diameters as a consequence. Thus at 25 °C, HAC shows a broad distribution with a significant maximum in the pore entry diameter close to 10^{-1} μm, whereas carbonated samples have this maximum displaced to between 10^{-1} and 10^{-2} μm. Table IV presents the cumulative volume measured for the samples tested. The total porosity is, not unexpectedly, influenced by conversion and is greatest at 55 °C. However, carbonated samples, even those cured and carbonated at 55 °C, have porosities not significantly different to unconverted, uncarbonated mortars cured at 5 °C.

3.3. Pore fluid analysis

The results of pore fluid analyses from HAC mortar with and without 3% NaCl addition after 21–23 days

TABLE IV Accessible porosity by mercury intrusion (maximum pressure, 2 GPa)

Sample	Temperature (°C)	Cumulative volume ($cm^3 g^{-1}$)
HAC	55	0.19
HAC	25	0.11
HAC	5	0.06
HAC +3 months CO_2	55	0.07
HAC +3 months CO_2	25	0.09
HAC +3 months CO_2	5	0.07

of curing at 5, 25 and 55 °C are presented in Table V. Despite the low alkali contents of HAC, relative to Portland cement, the pore fluids have high pHs, which are conditioned mainly by the aqueous Na and K. Under these conditions alumina is also relatively soluble. Addition of 3% NaCl increases pore fluid chloride contents, most markedly at 55 °C. As will be shown, much of the chloride originally in the mix water is bound as Friedel's salt at 5 °C. Friedel's salt is stable at 25 and 55 °C. However, at 55 °C, in the presence of alkali, the amount of Friedel's salt is greatly reduced. As a consequence, aqueous pore fluid chloride contents increase markedly at 55 °C relative to either 5 or 25 °C. Pore fluid pHs increase with sodium chloride additions and this higher pH correlates with higher levels of soluble alumina.

Table VI shows the pore fluid analyses after one and three months of carbonation. The last two columns of Tables V and VI, $\Sigma eq(+)$ $mol\,l^{-1}$ and $\Sigma eq(-)$ $mol\,l^{-1}$, calculate mass–charge balances of ions in solution. $\Sigma eq(-)$ * takes into consideration an estimation of the OH^- bonded to Al^{3+}, as in these cases it was not possible to titrate to a satisfactory end point with methyl orange. The overall charge balances are in reasonable agreement. The chemical mass balances can be subjected to further mathematical analysis which is presented in the discussion.

3.4. Differential thermal analysis and thermogravimetry

Fig. 2 shows an example of the thermograms obtained in paste samples; Table VII presents a summary of the different events found for paste samples cured for ~4 months and for paste samples carbonated for ~3 months. This severe regime was generally very effective in promoting carbonation, resulting in large amounts of normal hydrates being converted to $CaCO_3$ and $Al(OH)_3$, although exceptions were noted; some samples were remarkably resistant to carbonation.

3.5. Corrosion rate determination

The i_{corr} and E_{corr} values of steel bars embedded in mortar of HAC with and without NaCl are shown in Fig. 3 and 4 for three cure temperatures. After three weeks, i_{corr} values are below 0.1 $\mu A\,cm^{-2}$ and E_{corr} remains more positive than − 200 mV in plain mortars. These values indicate that the embedded steel is in a passive state. Higher cure temperatures enhance the

TABLE V Analysis of pore fluid of HAC pastes

Sample	Temperature (°C)	pH_e	pH_t (ph)	pH_t (m.o.)	Ca^{2+} (p.p.m.)	Al^{3+} (p.p.m.)	K^+ (p.p.m.)	Na^+ (p.p.m.)	Cl^- (p.p.m.)	$\Sigma eq(+)$ ($mol\,l^{-1}$)	$\Sigma eq(-)$ ($mol\,l^{-1}$)	$\Sigma eq(-)$* ($mol\,l^{-1}$)
~1 month cure												
HAC	55	12.68	13.04	13.26	3.2	627	1437	900	–	0.15	0.18	–
HAC	25	12.60	12.83	13.38	4.2	1090	1737	950	–	0.21	0.24	–
HAC	5	12.57	12.95	13.32	3.7	865	1312	794	–	0.16	0.21	–
HAC + 3% NaCl	55	12.81	13.44	13.73	0.9	2230	3094	38437	57900	2.00	2.17	–
HAC + 3% NaCl	25	13.16	14.00	14.44	0.3	13000	1937	32312	7350	2.90	2.96	–
HAC + 3% NaCl	5	13.13	13.95	14.28	0.5	8600	1344	21250	10500	2.00	2.19	–
~4 months cure												
HAC	55	–	12.94	–	5.0	472	1430	1230	< 30	0.14	0.09	0.16
HAC	25	–	12.99	–	15.5	1197	1580	1310	< 30	0.23	0.10	0.27
HAC	5	–	12.96	–	20.0	1046	1465	1210	< 30	0.21	0.09	0.24
HAC + 3% NaCl	55	–	13.42	–	5.6	1570	1750	26500	34500	1.37	1.23	1.46
HAC + 3% NaCl	25	–	13.97	–	4.7	1900	1200	24000	7950	1.28	1.15	1.43
HAC + 3% NaCl	5	–	14.20	–	2.1	16400	2340	38125	11800	3.54	1.91	4.34

$pH_e = pH_{electrode}$; $pH_t = pH_{titrated}$; ph = phenolphthalein; m.o. = methyl orange.

TABLE VI Analysis of pore fluid of carbonated HAC pastes

Sample	Temperature (°C)	pH_e	pH_t (ph)	pH_t (m.o.)	Ca^{2+} (p.p.m.)	Al^{3+} (p.p.m.)	K^+ (p.p.m.)	Na^+ (p.p.m.)	Cl^- (p.p.m.)	$\Sigma eq(+)$ ($mol\,l^{-1}$)	$\Sigma eq(-)$ ($mol\,l^{-1}$)	$\Sigma eq(-)^*$ ($mol\,l^{-1}$)
15 days initial cure + ~1 month CO_2												
HAC	55	12.12	12.17	12.52	21.2	17	700	2500	3625*	0.13	0.13	–
HAC	25	10.73	11.69	12.45	2.3	59.3	237	387	–	0.03	0.03	–
HAC	5	11.43	12.27	12.81	1.4	375	219	387	–	0.06	0.06	–
HAC + 3% NaCl	55	8.08	–	12.00	875	8.2	1375	18750	51450	0.89	1.46	–
HAC + 3% NaCl	25	13.15	13.73	14.17	1.4	5375	1081	10312	6000	1.17	1.65	–
HAC + 3% NaCl	5	12.74	13.53	13.90	0.2	2900	547	9375	4950	0.74	0.93	–
15 days initial cure + ~3 months CO_2												
HAC	55	–	< 8	–	1040	5.5	420	4500	9200	0.26	0.26	0.26
HAC	25	–	11.70	–	3.5	64.5	130	216	35	0.02	0.006	0.015
HAC	5	–	12.20	–	3.7	82.0	180	315	98	0.03	0.013	0.025
HAC + 3% NaCl	55	–	11.30	–	1633	25.5	540	12325	21050	0.63	0.59	0.60
HAC + 3% NaCl	25	–	13.50	–	2.7	2680	620	12000	10100	0.84	0.60	1.00
HAC + 3% NaCl	5	–	12.40	–	9.3	8.3	205	6750	5950	0.30	0.19	0.19

$pH_e = pH_{electrode}$; $pH_t = pH_{titrated}$; ph = phenolphthalein; m.o. = methyl orange.

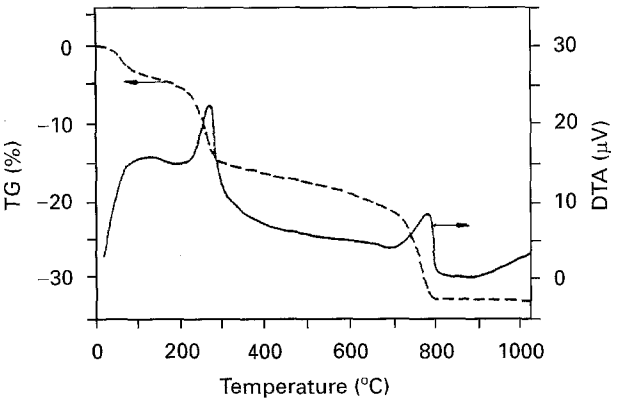

Figure 2 DTA and TG curves for HAC paste carbonated for ~3 months at 55 °C after 15 days of initial cure in 100% RH at 55 °C.

corrosion rates although i_{corr} values remain below 0.1 μA cm^{-2} throughout the test duration at all temperatures. The measured corrosion rates correspond to an average material loss, expressed as equivalent thickness of steel, of 5.8 μm in 50 years.

The results presented in Fig. 4 show that addition of 3% NaCl to the mix water is not sufficient to promote severe pitting corrosion of steel embedded in HAC mortar at 25 °C. Measured corrosion rates remain below 0.1 μA cm^{-2}, although increased by approximately one order of magnitude relative to those observed in mortars in the equivalent condition but without NaCl addition. When the cure temperature is decreased to 5 °C, measured i_{corr} values are typically about 1 μA cm^{-2}. The highest corrosion rates are observed at 55 °C; at this temperature the i_{corr} reaches about 5 μA cm^{-2} which corresponds to a material loss of ~3 mm in 50 years. The higher the values of corrosion rates, the more negative becomes the corrosion potential of embedded steel.

Figs 5 and 6 show the time dependence of i_{corr} and E_{corr} values for steel bars embedded in HAC mortar, with and without NaCl, which have also been carbonated at 5, 25 and 55 °C.

Fig. 5 shows that even after 3 months of carbonation at 5 and 25 °C, steel in HAC corrodes at rates below 0.1 μA cm^{-2} and E_{corr} values remain more positive than −200 mV. However, at 55 °C the passivation state is destroyed and corrosion rates are significantly higher than 1 μA cm^{-2}.

When steel is embedded in carbonated mortar formulated with 3% NaCl, corrosion rates are higher than in comparable mortars without chloride, as shown in Fig. 6. In the case of simultaneous carbonation with chloride addition, the final corrosion rates measured at 5 and 25 °C are about 0.3 μA cm^{-2}; this corresponds to a material loss of about 17.4 μm in 50 years with a further order of magnitude increase at 55 °C. These corrosion rates are broadly comparable to corrosion rates measured in uncarbonated mortars with 3% chloride addition at 55 °C.

4. Discussion

4.1. Solid phase

In commercial calcium aluminate cements, CA and, if present $C_{12}A_7$, are the only phases that hydrate

TABLE VII Thermogravimetric and differential thermal anlaysis data from HAC cements

Sample	Temperature (°C)	%$CaCO_3$ wt on ignited weight	T °C of peaks DTA
~4 months cure			
HAC	55	–	150, 295
HAC	25	–	150, 260, 290
HAC	5	3.1	130, 260, 710
HAC + 3% NaCl	55	–	150, 270, 300
HAC + 3% NaCl	25	–	130, 240–260, 300
HAC + 3% NaCl	5	3.2	130, 160, 190, 250, 690
15 d initial cure + ~3 months CO_2			
HAC	55	39.8	260, 770
HAC	25	19.8	260, 760
HAC	5	22.7	260, 760
HAC + 3% NaCl	55	30.5	260, 760
HAC + 3% NaCl	25	0	120, 160, 200, 250, 295
HAC + 3% NaCl	5	12.9	120, 180, 250, 730

Peaks at T < 200° C may be due to hexagonal hydrated aluminates.
Peak at ~300° C could be due to C_3AH_6 or AH_3 or both.
Peak at ~240–260° C may be due to F.S.
Peak at ~760–760° C is due to $CaCO_3$ decarbonation. The associated loss of weight has been used to evaluate the quantity of $CaCO_3$ in the sample and its degree of carbonation; the calculated % $CaCO_3$ is presented in the table.

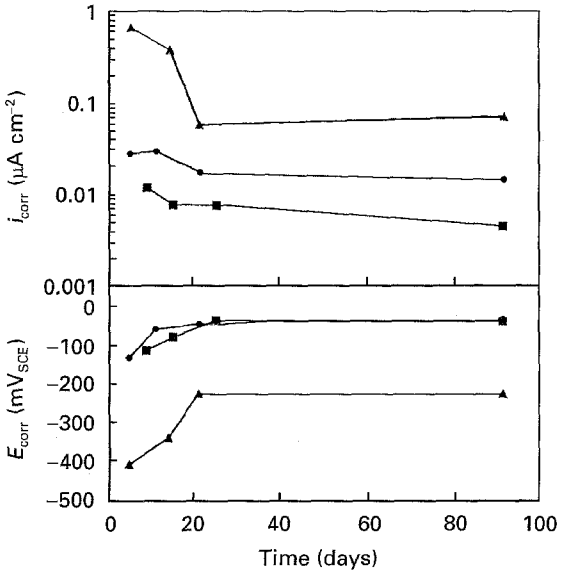

Figure 3 i_{corr} and E_{corr} values versus time for steel bars embedded in HAC mortar for three cure temperatures: 5(●), 25 (■) and 55 °C (▲).

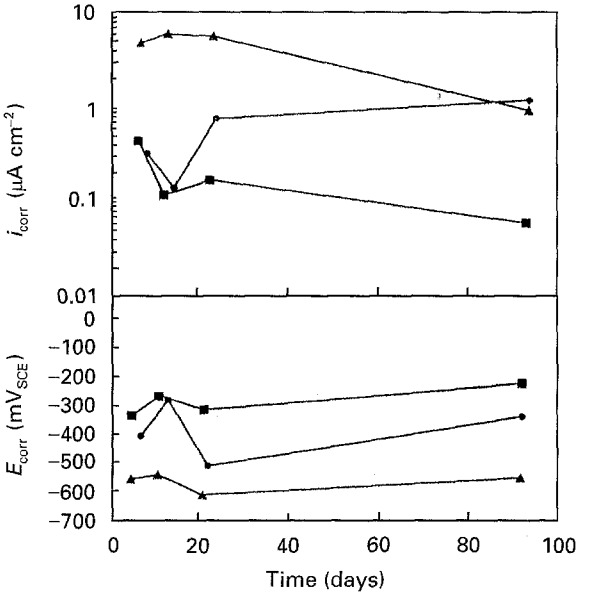

Figure 4 i_{corr} and E_{corr} values versus time for steel bars embedded in HAC mortar with 3% NaCl for three cure temperatures: 5 ●, 25 ■ and 55 °C ▲.

significantly at early ages: C_2S hydrates more slowly. The hydration of monocalcium aluminate has been studied extensively. It is generally observed that the hydrates formed depend on temperature:

- at low temperatures below 15 °C, CAH_{10} is the main hydrate found
- at temperatures between 15 and 30 °C, CAH_{10} occurs in mixtures with C_2AH_8 and AH_3 gel.
- at temperatures above 30 °C, C_2AH_8 and AH_3 are formed together but convert rapidly at 30 °C and very rapidly, if not simultaneously, above 45 °C to mixtures of C_3AH_6 and gibbsite, $Al(OH)_3$.

Observations made in the course of the present study agree with those in the literature; the major hydrated aluminates, after initial cure, are CAH_{10} at 5 °C, mixtures of CAH_{10} and C_2AH_8 at 25 °C and C_3AH_6 with AH_3 at 55 °C. The completion of hydration is slow; unhydrated CA still persists after 4 months at 5 °C. The retardation of hydration at low temperature is more pronounced when chloride is present. NaCl forms Friedel's salt and, although the amount of chloride added is insufficient to convert more than a fraction of the total aluminates to Friedel's salt, its formation apparently inhibits the overall hydration kinetics.

The conversion of the remaining unstable hexagonal hydrated phases (CAH_{10}, C_2AH_8, etc.) to more stable cubic phase takes place in chloride-containing samples after 3 months of carbonation at 25 °C. This cylinder has a very low degree of carbonation; it has

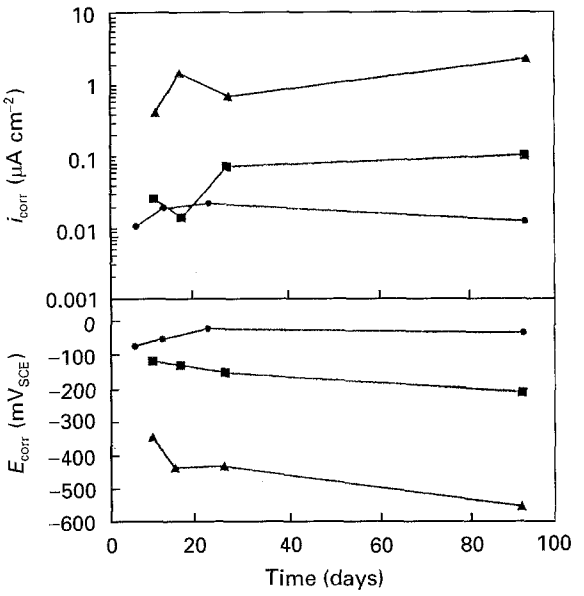

Figure 5 i_{corr} and E_{corr} values versus time for steel bars embedded in HAC mortar carbonated for three cure temperatures: 5 (●), 25 (■) and 55 °C (▲).

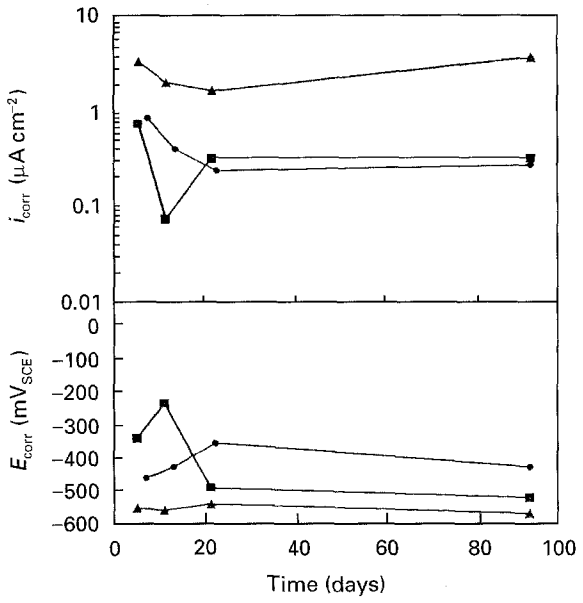

Figure 6 i_{corr} and E_{corr} values versus time for steel bars embedded in HAC mortar with 3% NaCl carbonated for three cure temperatures: 5 (●), 25 (■) and 55 °C (▲).

practically zero $CaCO_3$ on the ignited weight (see Table VII) and retains a pore fluid pH = 13.5 (see Table VI). Despite a high initial w/c ratio, it is very resistant to carbonation.

The formation of crystalline gehlenite hydrate, C_2ASH_8, was also detected in samples kept at 5 °C; that is, in the sample which had the slowest hydration reaction rate for aluminates. Hence silicate is presumably able to contribute to space-filling of the hydrated paste matrix. This, in turn, is believed to retard the kinetics of subsequent carbonation at ~25 °C.

The degree of carbonation tends to be highest following elevated temperature cure: that is, in the more porous samples cured at 55 °C. However, low temperature cure can make the paste remarkably resistant to carbonation, even when formulated to a relatively high w/c ratio; even after 3 months in CO_2, the bulk of a HAC + 3% NaCl mortar remained essentially uncarbonated at 25 °C.

4.2. Pore solution phase

The kinetics of hydration of both HAC and monocalcium aluminate, and the composition of the aqueous phase in equilibrium with the solid phase have been studied previously [5–8]. The composition of the aqueous solution obtained immediately after mixing tends to be controlled by the nearly congruent solubility of CA, which typically produces an aqueous C/A ratio of 1.12 and pH of 11.56. Commercial cements reflect similar chemical balances during early hydration: during the induction period, the C/A ratio is typically ~0.95 and the pH ~11.5. The main changes in the composition of pore solutions takes place once the induction period ends; massive precipitation of hydrated aluminates occurs, alkalis are released from clinker phases and increasing aqueous Na and K contents markedly elevate the pH. In response to these changes, aqueous Ca^{2+} concentrations decrease.

The volume of the aqueous pore phase is of course not constant over hydration time but decreases progressively as formation of the hydrated phases occurs. This decrease in the volume of the aqueous phase influences the concentrations of ionic species making it apparently impossible to establish the net movement of the ions between solid and liquid phases. To help solve this problem, a water concentration factor has been introduced [8]. This procedure was used in the present investigation for a few specimen calculations.

When the anhydrous phases react with water the species present in solution in significant concentrations are Ca^{2+}, $Al(OH)_4^-$, Na^+, K^+, OH^-, and Cl^-, if NaCl has been added. Table VIII presents proof that the main speciation of aluminium in solution is $Al(OH)_4^-$. In this table, the ratio Z/Al^{3+} is calculated from experimental results, Z being the difference between the $[OH^-]$ measured with phenolphthalein and methyl orange, that is the $[OH^-]$ which is co-ordinated to aluminium in solution. This Z value is close to 4, indicating Al is co-ordinated by an average of 4 OH^- in uncarbonated pore fluids. However, Z increases to values greater than 4.0 as the paste is progressively carbonated. The increase is attributed to changes in aluminium co-ordination, perhaps to octahedral, in response to the lower pH developed as carbonation progresses.

The pore fluid compositions from uncarbonated pastes analysed in the present work have been extracted from samples cured for at least 21–23 days, by which time aqueous CaO/Al_2O_3 ratios are low (see Table IX). Progressive solubilization of cement alkalis strongly increases aqueous Na^+ and K^+ concentrations and pH; indeed, in common with Portland cement and its blends the pH of the pore phase is dominated by the alkali concentrations [9]. Table IX presents pH values calculated from experimentally determined Na^+ and K^+ concentrations, subtracting

TABLE VIII Ratio Z/Al^{3+} for pore fluids of HAC pastes. (Z being the difference between the $[OH^-]$ measured with phenophthalein and methyl orange, that is the $[OH^-]$ which is co-ordinated to aluminium in solution)

Sample	Temperature (°C)	~ 1 month cure	15 days initial cure + ~ 1 month CO_2
HAC	55	3.47	30.00[a]
HAC	25	4.30	9.50
HAC	5	3.75	3.28
HAC +3%NaCl	55	3.17	33.33
HAC +3%NaCl	25	3.65	4.33
HAC +3%NaCl	5	3.19	4.02

[a] Sample contaminated with chloride.

TABLE IX Pore fluid analyses and chemical balances in HAC cements cured under various conditions

Sample	Temperature (°C)	$pH_{exp.}$	$pH_{theor.}$	Na^+(M)	K^+ (M)	$CaO/Al_2O_3 \times 10^{-3}$
~ 1 month cure						
HAC	55	13.04	12.87	0.039	0.036	1.7
HAC	25	12.83	12.92	0.041	0.044	1.2
HAC	5	12.95	12.82	0.034	0.033	1.4
HAC +NaCl	55	13.44	13.07	0.038	0.079	0.1
HAC +NaCl	25	14.00	14.09	1.198	0.049	0.01
HAC +NaCl	5	13.95	13.82	0.628	0.034	0.02
15 days initial cure + ~1 month CO_2						
HAC	55	12.17	12.36	0.006	0.017	415
HAC	25	11.69	12.34	0.016	0.006	13
HAC	5	12.27	12.32	0.016	0.005	1.2
HAC +NaCl	55	8.08	–	$Cl^- > Na^+$	0.035	36385
HAC +NaCl	25	13.73	13.48	0.279	0.027	0.08
HAC +NaCl	5	13.53	13.45	0.268	0.014	0.02
~ 4 months cure						
HAC	55	12.94	12.94	0.053	0.036	3.6
HAC	25	12.99	12.98	0.056	0.040	4.3
HAC	5	12.96	12.94	0.052	0.037	6
HAC +NaCl	55	13.42	13.34	0.179	0.044	1.2
HAC +NaCl	25	13.97	13.92	0.819	0.030	0.8
HAC +NaCl	5	14.20	14.14	1.326	0.059	0.04
15 days initial cure + ~3 months CO_2						
HAC	55	< 8	–	$Cl^- > Na^+$	0.010	64870
HAC	25	11.70	12.04	0.008	0.003	18
HAC	50	12.20	12.17	0.011	0.004	1150
HAC +NaCl	55	11.30	–	$Cl^- > Na^+$	0.014	21670
HAC +NaCl	25	13.50	13.40	0.237	0.015	0.3
HAC +NaCl	5	12.40	13.11	0.125	0.005	370

from the total Na the equivalent required to charge balance the chloride. Despite the potential for error inherent in the procedure, generally good agreement between calculated and experimental pH values are observed. The isothermal pH of commercial HAC pore fluids are thus determined primarily by the alkali content of the cement and are independent of the type of hydrated aluminates formed. In this study, the intrinsic pH of uncarbonated or lightly carbonated matrices is about 13 at all cure temperatures tested over the duration of the test. These conditions are quite general and do not depend primarily on the original w/c ratio and hence the amount of pore fluid, although the w/c ratio will have a secondary influence on the exact numerical values. Had the cement been made to low w/c ratio, as good practice demands, the observed pore fluid alkali concentrations would be higher than reported here.

4.3. Stability of the solid phases

The different hydrates detected from XRD data (C_3AH_6, C_2AH_8 and CAH_{10}) are believed to reach a solubility equilibrium after one month. Using the following solubility product expressions enables further calculations to be made

$$C_3AH_6 \rightleftarrows 3Ca^{2+} + 2Al(OH)_4^- + OH^-$$

$$\log K_s = -22.3$$

$$C_2AH_8 \rightleftarrows 2Ca^{2+} + 2Al(OH)_4^- + 2OH^-$$

$$\log K_s = -13.8$$

$$CAH_{10} \rightleftarrows Ca^{2+} + 2Al(OH)_4^-$$

$$\log K_s = -7.6$$

The solubility products, calculated from the experimental concentrations of ions present in pore phase,

TABLE X Phase solubility calculations for HAC cements cured under various conditions

Sample	Temperature (°C)	I(M)	$\log K_s C_3AH_6$	$\log K_s C_2AH_8$	$\log K_s CAH_{10}$
~ 1 month cure					
HAC	55	0.104	− 21.5	–	–
HAC	25	0.098	–	− 14.4	− 7.4
HAC	5	0.096	–	–	− 7.6
HAC + NaCl	55	1.868	− 20.4	–	–
HAC + NaCl	25	1.572	–	− 12.4	− 6.5
HAC + NaCl	5	1.231	–	–	− 6.7
15 days initial cure + ~1 month CO_2					
HAC	55	0.120	− 26.3	–	–
HAC	25	0.015	–	− 14.5	− 9.8
HAC	5	0.028	–	–	− 8.5
HAC + NaCl	55	1.194	− 44.3	–	–
HAC + NaCl	25	0.692	–	–	− 6.8
HAC + NaCl	5	0.504	–	–	− 8.2
~ 4 months cure					
HAC	55	0.099	− 21.4	–	–
HAC	25	0.121	− 18.7	–	− 6.8
HAC	5	0.110	–	–	− 6.8
HAC + NaCl	55	1.244	− 18.9	–	–
HAC + NaCl	25	1.149	–	− 12.0	− 7.1
HAC + NaCl	5	2.119	–	–	− 6.1
15 days initial cure + ~3 months CO_2					
HAC	55	0.284	− 38.8	–	–
HAC	25	0.011	–	− 18.5	− 9.6
HAC	5	0.017	–	–	− 9.4
HAC + NaCl	55	0.654	− 23.9	–	–
HAC + NaCl	25	0.621	− 19.4	− 13.3	− 7.1
HAC + NaCl	5	0.243	–	–	− 11.5

are presented in Table X. Activity coefficients γ have been calculated using the extended Debye–Hückel expression

$$\log \gamma = -0.51\, z_i^2\, I^{\frac{1}{2}}/(I + I^{\frac{1}{2}}) + 0.2\, I \quad (1)$$

where z is the charge of the ion and I is the ionic strength of the solution.

From the experimental $\log K_s$ values, it is deduced that pore fluids are broadly in thermodynamic equilibrium with the solid phases detected by XRD. However, when the aqueous phase uptakes carbonate, pore solutions become undersaturated with respect to the normal solid hydrate phases i.e. they are calculated to become unstable. This is clearly confirmed by X-ray diffractograms in which hydrated calcium aluminate phases are no longer detected in fully carbonated regions.

4.4. Binding of chloride and alkalis

Addition of 3% of NaCl to mix water produces a marked increase in pore fluid pH. This arises because the cement solids bind chloride, leaving OH^- as the only soluble species to charge balance the alkali. However, this pH increase is less important for samples cured at 55 °C, because of the decreasing capacity of the paste to bind chloride decreases; as less chloride is bound, the charge on soluble alkalis is increasingly compensated by dissolved chloride, instead of OH^-, with the result that the increase in pH is no longer proportional to the increase in alkali concentration.

The potential capacity of HAC to fix Cl^- in the form of Friedel's salt has been reported previously [2]. This compound is detected by X-ray diffraction in all samples containing chloride, although its relative amount does not correlate simply with the chloride concentration of the coexisting pore fluid, probably because a significant amount of chloride also substitutes for OH^- in the hexagonal hydroxy AFm hydrates: Friedel's salt only appears after some threshold concentration necessary for its stabilization is exceeded. In fact, 3% NaCl is sufficient to stabilize at least some Friedel's salt in pastes at all temperatures although, as noted, samples cured at 55 °C have higher concentrations of Cl^- in pore fluid because of the diminished amounts of Friedel's salt. The NaCl concentration added corresponds to an initial Cl^- concentration of about 30 000 p.p.m. in the mix water. Some of the liquid water is, of course, bound into hydrate product. If a water concentration factor of 3 is assumed [7, 8] and if all chlorides were to remain in the aqueous phase, its concentration in pore fluids would be expected to rise to ~90 000 p.p.m. This is of course much higher than was measured experimentally; (see Table VI) the reduction in pore fluid concentration may, very roughly, be taken as a measure of the quantitative extent to which chloride binding occurs in cement paste solids.

Finally it is important to point out that the pH value of HAC pore fluid phase is not necessarily less than that of a Portland cement. Although Portland cements typically have the higher alkali contents, their

solids – particularly C–S–H – also have greater sorption capacity for alkali, with the result that alkalis in HAC, which typically have low C–S–H contents, concentrate to a greater extent in pore fluid. However, HACs are likely to vary considerably in alkali binding potential insofar as their capacity to bind alkali is related to C–S–H contents. Some HAC clinkers contain silica combined as C_2S; these have the greatest capacity for C–S–H formation and are likely to have the best capacity to bind alkalis into cement solids.

4.5. Corrosion behaviour of steel embedded in HAC

The corrosion rates of steel in HAC mortars in all the conditions tested are shown in Fig. 7. Corrosion data can also be correlated with other physical features of the paste, e.g. cumulative porosity and chemical factors, and also extent of carbonation and free chloride. The data cannot embrace all conditions of exposure likely to be encountered in real situations, but are representative of the corrosion tendency of steel under a range of defined conditions. Results of porosity, degree of carbonation and chloride concentrations are also given. From this figure the following conclusions can be drawn:

- For plain HAC, the corrosion rate of steel depends mainly on paste porosity and temperature. Diffusion of oxygen may be the rate-controlling factor.
- For HAC with chloride addition, the steel corrosion rate is directly related to pore fluid chloride content; that is, the higher the chloride concentration, the higher the corrosion rates. However, chloride contents are significantly lowered by incorporation into the aluminates. In this respect, the chloride binding power of HAC exceeds that of OPC.
- For partially carbonated HAC matrices, the corrosion rate increases at $> 30\%$ $CaCO_3$, at which point the pH value is lower than 12.

In summary, steel embedded in HAC mortar behaves normally and follows the general principles of corrosion science. For mortar without chloride addition and with a pore fluid pH above 12.5, steel is in a passivated state and measured corrosion rates are $< 0.1\ \mu A\ cm^{-2}$.

4.6. Origin of chloride and initiation of corrosion

Much discussion of corrosion behaviour centres about the source of corrosion initiators. In a realistic situation, the concrete cover would be expected to have a low intrinsic chloride content, with chloride reaching embedded steel from an external source. On the other hand, experimenters generally add chloride to the paste, both to ensure reproducible experimental measurements and to accelerate the experiments. The question may be asked: do laboratory simulations adequately reflect practice?

The presence of chloride tends to destroy the passivation state of steel; a pitting corrosion regime develops with the result that measured corrosion rates are

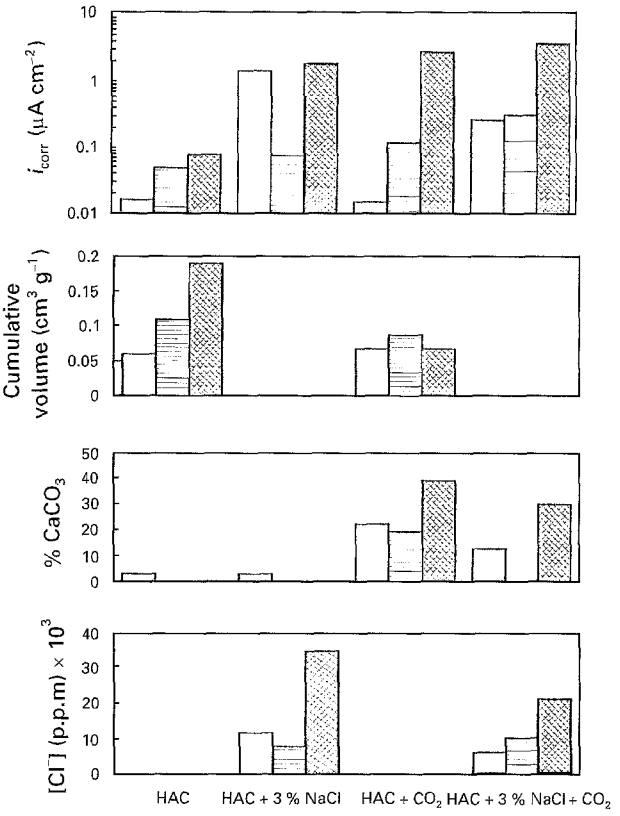

Figure 7 Final corrosion rates of steel in HAC mortar, porosity, degree of carbonation and chloride content of pore fluid in all the conditions tested. □ 5, ▤ 25, ▩ 55 °C.

higher than $1\ \mu A\ cm^{-2}$. However, the relevant chloride ions are those which have reached the steel/cement interface. Solid phases of HAC pastes, by binding chloride ions, increase the effectiveness of cover concrete in protecting steel relative to OPC mixes, but even when chloride is present at the interface with steel, for example, in the HAC + 3% NaCl sample, the steel still exhibits a low corrosion rate of $0.1\ \mu A\ cm^{-2}$. Although higher corrosion rates are measured for carbonated, chloride- containing samples, even these rates are not excessive. Moreover, good quality HAC mortar can be very resistant to carbonation. Perhaps reflecting these observations, no signs of cracking or physical distress were noted in any of the tests samples. It is therefore concluded that laboratory simulants do adequately reflect the behaviour of uncracked cover concrete but eliminate the need for a time-consuming diffusion stage.

4.7. Behaviour of HAC in chemically-complex chloride solutions

The present results show good dimensional stability and resistance to carbonation of NaCl-containing HAC formulations. This accords with decades of experience. Clearly, however, there are limits of chloride concentrations and combinations of chloride with cations which may be inimical to HAC. For example, Kurdowski and co-workers [10] describe the mineralogical and microstructural changes to high alumina cements immersed in NaCl-containing solutions containing 14, 195 and 240 g/l for two years; other salts present were $MgCl_2$, KCl and $MgSO_4$. The

paste cubes had generally good durability. However, the attacking aqueous phase was chemically complex and many of the dimensional changes and precipitated phases related to the presence of salts other than NaCl. For example, basic magnesium chlorides formed even though the maximum $MgCl_2$ concentration of the brine was only 3 $g l^{-1}$. Thus it is important to extend the data to include a range of natural-water chemistries if a fuller understanding of the corrosion behaviour is to be obtained.

5. Conclusion

Eventually, chloride will penetrate to the steel. When this occurs, experiments made by adding NaCl to the mix water have relevance. Low corrosion rates are observed in the absence of ready access by oxygen to the paste-steel interface.

The resistance of HAC to carbonation and its greater potential for chloride binding by chloroaluminate formation are believed to make HAC inherently more protective to steel, relative to normal Portland cement, during ingress of chloride from external sources.

High corrosion rates reported in the literature for steel embedded in HAC may be attributable to bad practice, not to lack of passivity.

Acknowledgements

A. Macias gratefully acknowledges: financial support received from the Comunidad Autónoma de Madrid and the DGICYT, the Department of Chemistry of the University of Aberdeen and the Instituto Eduardo Torroja of Construction Science, for the provision of laboratory facilities.

References

1. A. J. MAJUMDAR, R. N. EDMONDS and B. SINGH, in "Calcium aluminate cements", edited by R. J. Mangabhai (E & FN Spon, London 1990) p. 259.
2. M. PÉREZ, F. TRIVIÑO and C. ANDRADE, *Mater. de Const.* **182** (1981) 49.
3. S. GOÑI, C. ANDRADE and C. L. PAGE, *Cem. Concr. Res.* **21** (1991) 635.
4. M. STERN and A. L. GEARY, *J. Electrochem. Soc.* **104** (1957) 56.
5. P. BARRET, D. MÉNÉTIER ET D. BERTRANDIE, *Cem. Concr. Res.* **4** (1974) 545.
6. D. BERTRANDIE ET P. BARRET, in Proceedings of the 7th International Symposium on the Chemistry of Cement, Paris, (1980) p. 79.
7. K. FUJII, W. KONDO and H. UENO, *J. Amer. Ceram. Soc.* **69** (1986) 361.
8. MA. T. GAZTAÑAGA, S. GOÑI and J. L. SAGRERA, *Mater. de Const.* **42** (1992) 65.
9. S. DIAMOND, *Cem. Concr. Res.* **11** (1981) 383.
10. W. KURDOWSKI, L. TACZUK and B. TSRYBVALSKA, in "Calcium aluminate cements", edited by R. J. Mangabhai (E & FN, Spon, London, 1990) p. 222.

Received 21 August
and accepted 4 October 1995